

Published in final edited form as:

*Biomaterials*. 2009 December ; 30(35): 6748–6756. doi:10.1016/j.biomaterials.2009.08.042.

## Magnetic Resonance Imaging of Multifunctional Pluronic Stabilized Iron-Oxide Nanoparticles in Tumor-Bearing Mice

Tapan K. Jain<sup>1,#,†</sup>, Susan P. Foy<sup>1,#</sup>, Bernadette Erokwu<sup>2</sup>, Sanja Dimitrijevic<sup>1</sup>, Christopher A. Flask<sup>2</sup>, and Vinod Labhasetwar<sup>1,3,\*</sup>

<sup>1</sup>Department of Biomedical Engineering, Lerner Research Institute, Cleveland Clinic, Cleveland, OH 44195, USA

<sup>2</sup>Department of Radiology, Case Center for Imaging Research, Case Western Reserve University, Cleveland, OH 44106, USA

<sup>3</sup>Taussig Cancer Institute, Cleveland Clinic, Cleveland, OH 44195, USA

### Abstract

We are investigating the magnetic resonance imaging characteristics of magnetic nanoparticles (MNPs) that consist of an iron-oxide magnetic core coated with oleic acid (OA), then stabilized with a pluronic or tetronic block copolymer. Since pluronics and tetronics vary structurally, and also in the ratio of hydrophobic (poly[propylene oxide]) and hydrophilic (poly[ethylene oxide]) segments in the polymer chain and in molecular weight, it was hypothesized that their anchoring to the OA coating around the magnetic core could significantly influence the physical properties of MNPs, their interactions with biological environment following intravenous administration, and ability to localize to tumors. The amount of block copolymer associated with MNPs was seen to depend upon their molecular structures and influence the characteristics of MNPs. Pluronic F127-modified MNPs demonstrated sustained and enhanced contrast in the whole tumor, whereas that of Feridex IV was transient and confined to the tumor periphery. In conclusion, our pluronic F127-coated MNPs, which can also be loaded with anticancer agents for drug delivery, can be developed as an effective cancer theranostic agent, i.e. an agent with combined drug delivery and imaging properties.

### Keywords

Magnetic Nanoparticles; Tumor Detection; Block Copolymers; Magnetic Resonance Imaging

### 1. Introduction

Magnetic resonance imaging (MRI) provides excellent differential soft-tissue contrast in order to discriminate between healthy tissue and abnormalities such as tumors. Contrast agents further improve tissue resolution obtained with MRI by influencing the properties of the

© 2009 Elsevier Ltd. All rights reserved.

\*Author for correspondence: Vinod Labhasetwar, Ph.D., Department of Biomedical Engineering/ND20, Cleveland Clinic, 9500 Euclid Avenue, Cleveland, OH 44195, Tel: 216/445-9364, Fax 216/444-9198, labhasv@ccf.org.

<sup>#</sup>TKJ and SPF contributed equally to this work.

<sup>†</sup>Current Affiliation: University School of Basic & Applied Sciences, Guru Gobind Singh Indraprastha University, Kashmere Gate, Delhi-110403, India

**Publisher's Disclaimer:** This is a PDF file of an unedited manuscript that has been accepted for publication. As a service to our customers we are providing this early version of the manuscript. The manuscript will undergo copyediting, typesetting, and review of the resulting proof before it is published in its final citable form. Please note that during the production process errors may be discovered which could affect the content, and all legal disclaimers that apply to the journal pertain.

adjacent tissue. Several different types of contrast agents exist: paramagnetic gadolinium agents brighten the tissue by increasing the longitudinal relaxivity, whereas superparamagnetic nanoparticles darken the tissue by altering the transverse relaxivity [1]. In oncology, magnetic nanoparticles (MNPs) are being used to aid in disease staging, treatment planning, and assessing tumor response to therapy [2,3]. In particular, MNPs are increasingly being used for nodal staging because of their uptake by macrophages and migration to the lymph nodes [3]. Additionally, the enhanced permeation and retention (EPR) effect can be utilized to increase MNP uptake in the tumor for MRI; however, MNPs for this purpose must be appropriately designed to avoid their uptake by macrophage, resulting in rapid clearance from the systemic circulation [4].

To address the problems of short half-life and rapid clearance by the reticuloendothelial system (RES), MNPs are modified with various surface coatings, such as dextran, starch, citrate or synthetic polymers [1]. The surface coating affects the hydrodynamic diameter of the MNPs and their interaction with proteins circulating in the bloodstream, both of which lead to opsonization, macrophage uptake, and clearance by the RES [5]. By altering the surface coating, it is possible to limit MNP interaction with the surrounding environment after intravenous administration and prevent uptake by the RES, influencing the systemic circulation time and eventual localization efficiency of the MNPs to the tumor [6].

We have developed an innovative MNP formulation that consists of an iron-oxide magnetic core, which is coated with oleic acid (OA) and then stabilized with a block copolymer, rendering the formulation dispersible in water and suitable for intravenous administration [7]. In the present study, we examined the effects of different pluronic and tetronic block copolymers on the characteristics of MNPs. The pluronic block copolymer consists of a hydrophobic poly(propylene oxide) (PPO) chain flanked on each side with hydrophilic poly(ethylene oxide) (PEO) chains. Tetronic block copolymers contain four PPO-PEO chains connected together at the PPO subunits to form a star shape structure (Fig. 1). Different pluronics and tetratics vary structurally, as well as in the ratio of hydrophobic PPO and hydrophilic PEO segments in the polymer chain and in molecular weight (Table 1). Thus, we hypothesized that how well these block copolymers anchored to the OA coating could significantly influence the properties of the MNPs (e.g., particle size, protein binding and binding constant, dispersion stability in phosphate-buffered saline [PBS], and macrophage uptake). These properties of MNPs are important, as they could also influence the interactions of MNPs with the RES. Such interactions could influence the systemic circulation time of MNPs and their localization efficiency in the tumor. The results of the *in vitro* experiments were used to rationally decide which MNP formulations would work best *in vivo* for imaging in tumor-bearing mice. We compared our formulations with that of a commercially available dextran-coated iron-oxide MNP, Feridex IV.

## 2. Materials and Methods

### 2.1 Materials

Pluronics (F127, F68, F108, and L64) and Tetratics (T904 and T908) were a gift from BASF Corporation (Mt. Olive, NJ). Feridex IV was purchased from Berlex Laboratories (Montville, NJ). Deionized water freshly purged with nitrogen gas was used as described below in all of the steps involved in MNP synthesis.

### 2.2 Synthesis and characterization of magnetic nanoparticles

Iron-oxide nanoparticles were prepared by co-precipitation of Fe(III) and Fe(II) with ammonium hydroxide. Three milliliters of 5 M ammonium hydroxide was added dropwise over 1 min to a mixture of 0.1 M Fe(III) (30 mL) and 0.1 M Fe(II) (15 mL) while stirring on

a magnetic stir plate. The mixture was stirred for 20 min under a nitrogen-gas atmosphere, and 100 mg of OA was added. The mixture was heated to 80°C for 30 min while being stirred and then cooled down to room temperature. The OA-coated iron-oxide NPs were separated by placing a magnet (12,200 G, Edmund Scientific, Tonawanda, NY) below the beaker for 5 min, and the resulting supernatant was discarded. The separated OA-magnetite particles were washed three times with water by magnetic separation and resuspended in 45 mL of water. To prepare MNPs with different pluronics and tetronics, 100 mg of each one of the block copolymers was added to OA-magnetite particles prepared as above, and the particle suspension was kept overnight under constant magnetic stirring. The MNP suspension was washed three times using magnetic separation and centrifuged at 1,000 rpm for 15 min at 10°C to remove large aggregates. The ratio of OA to pluronic F127 was optimized in our previous studies to obtain small MNPs with a low polydispersity index [7]. This amount of block copolymer is in excess of what can bind to the MNPs, so we used 100 mg of each of the different block copolymers for surface modification of the MNPs.

The iron content of the MNPs was estimated using the 1,10 phenanthroline colorimetric method [8]. Dynamic laser light scattering with the NICOMP™ 380 ZLS (Particle Sizing Systems, Santa Barbara, CA) was used to measure the mean hydrodynamic particle size of the MNPs, comparing different pluronic or tetronic coatings in water, PBS, 0.1% bovine serum albumin (BSA, Fraction V, Sigma-Aldrich, St. Louis, MO) in water, and mannitol-citrate buffer, pH 7.4. The size of the iron-oxide core of the MNPs was determined using a Philips 201 transmission electron microscope (Philips/FEI Inc., Briarcliff, Manor, NY). Samples were heated at the rate of 20°C/min under 20 mL/min nitrogen gas flow to obtain a thermogram for each sample between 30°C and 1000°C. Lyophilized samples were used to confirm the adsorption of the pluronic and tetronic block copolymer coatings with a Fourier transform infrared (FTIR) spectrometer (PerkinElmer LLC, Shelton, CT), and to determine the OA and pluronic or tetronic content of the MNPs by thermogravimetric analysis (Pyris 1 TGA, PerkinElmer LLC, Shelton, CT).

### 2.3 Protein binding studies and magnetic nanoparticle uptake by macrophage cells

Each MNP formulation was studied for binding to BSA using fluorescence spectroscopy. The BSA solution (330 µg/mL, in mannitol-citrate buffer) was titrated with 1 mg/mL aliquots of MNP suspension such that the total protein concentration remained less than 2%. The fluorescence emission spectra of BSA at different MNP concentrations was recorded at the excitation wavelength,  $\lambda_{\text{ex}} = 295$  nm and over emission wavelengths of 300–500 nm using a fluorescence spectrophotometer (PerkinElmer Life and Analytical Sciences, Inc, Waltham, MA). The intrinsic fluorescence of tryptophan residues in BSA is quenched on binding to specific sites of MNPs. This characteristic provides a method to determine binding constant ( $K_b$ ) and number of binding sites ( $n$ ) (Supplementary Fig. S1), according to the methods of Lehrer and Fasman [9] and Chipman et al. [10].

The mouse leukemic monocyte macrophage cell line RAW 264.7 was maintained in RPMI 1640 medium supplemented with 10% fetal bovine serum, 100 mg/mL penicillin G, and 100 mg/mL streptomycin at 37°C in a humidified and 5% CO<sub>2</sub> atmosphere. Macrophage cells were seeded in 6-well plates (200,000 cells per well) and allowed to reach ~80% confluency. Medium was replaced with 0.1 mg/mL MNP suspensions in media (2 ml/well) and incubated for 4 h at 37°C. After 4 h, macrophage cells were washed gently two times with PBS, the cells were scraped and centrifuged (1000 rpm, 10 min), and the resulting pellet was used to determine MNP uptake. With concentrated hydrochloric acid added, the cell pellet was incubated at 37°C for 30 min, and the resulting solution was diluted for iron estimation [8]. Calibration curves for each formulation were prepared by plotting a known concentration of MNPs and measuring the absorbance at 511 nm. A portion of cell suspension was lysed using 1% Triton X 100

(Sigma), and protein estimation performed using a bicinchoninic acid protein assay kit (Pierce, Rockford, IL).

## 2.4 Tumor inoculation in athymic mice

All procedures involving live animals were approved by the Cleveland Clinic Institutional Animal Care and Use Committee. We have developed a new method of tumor induction that forms tumors of consistent size and in which more animals develop tumors than by the conventional method of tumor induction using cells in Matrigel™ (BD Biosciences, Bedford, MA) alone. In our study, cancer cells are first grown onto a poly(lactide)-based scaffold designed in our laboratory into a three-dimensional tumor-like structure and then combined with Matrigel™ prior to inoculation [11]. Athymic nude mice (20- to 30-g females, nu/nu, Charles River, Wilmington, MA) were anesthetized by intraperitoneal injection of 100–150 mg/kg body weight of ketamine and 10 mg/kg xylazine. Each mouse was injected with 500,000 MCF-7 cells grown on scaffold in a 100- $\mu$ l mixture of D-PBS and 100- $\mu$ l Matrigel™ in the upper rightmost mammary gland. A 17- $\beta$ -estradiol pellet (1.5 mg, 60-d release; Innovative Research of America, Sarasota, FL) was implanted subcutaneously in the left flank of each mouse.

## 2.5 Magnetic resonance imaging

Magnetic resonance imaging studies were done when the mean tumor volume reached  $\sim 250$  mm<sup>3</sup>. During imaging, mice were anesthetized with isoflurane and their temperature and respiration were monitored for the duration of the experiment. A phantom (syringe filled with water) was placed alongside the mouse during imaging and used for image normalization. The tail vein was catheterized using a 26-gauge needle connected to PE20 tubing that had been flushed with heparinized saline. A suspension of MNPs or Feridex IV (40 mg Fe/kg,  $\sim 100$   $\mu$ L) in mannitol-citrate isotonic solution was injected through the tail vein over 40 sec. Mannitol-citrate buffer (100  $\mu$ L) was used as a control.

Dynamic scanning of mice was performed using a 9.4 T Bruker Biospec MRI scanner (Bruker Biospin, Billerica, MA) to observe the changes in the signal intensity in the tumor following administration of the contrast agents. A dynamic FLASH acquisition (TR/TE = 221.4/2.1 ms, field of view = 3.0 $\times$ 3.0 cm, matrix = 256 $\times$ 256, alpha = 20°, slice thickness = 1 mm) was used to acquire images of the tumor for each animal. After 3–4 pre-injection FLASH scans, the mouse was removed from the MRI scanner and injected with either saline, Feridex IV, or F127- or T908-modified MNPs. This step was performed so that the MNPs could be injected without aggregating in the PE20 tubing due to the magnetic field of the MRI scanner. The animal was then placed back at the same axial distance with the scanner, and the tumor imaged at 1, 2.5, 3, and 4 h post-injection of the contrast agent.

Preliminary tumor studies were analyzed for changes in signal intensity with Amira software (Mercury Computer Systems, Chelmsford, MA). Subsequent studies were analyzed with MATLAB (The MathWorks, Natick, MA), as stated in the figure legends. The images acquired were normalized with respect to the noise and the phantom according to the following equation: Normalized Image = (Original Image – Noise)/(Phantom – Noise). Two regions of interest (ROIs) were manually drawn for each tumor slice, one surrounding the whole tumor, and the other just inside the tumor periphery (Supplementary Fig. S2). The signal intensities within the whole tumor and within the hollow tumor periphery were determined using the same ROI at each time point. This process was repeated for each tumor slice (7–8 slices per tumor), and an area weighted average was calculated over the whole tumor volume.

## 2.6 Histological analysis

Tumors were collected 24 h after injection of the contrast agent. Mice were deeply anesthetized with an intraperitoneal injection of sodium pentobarbital (150 mg/kg), then perfused with PBS and 4% paraformaldehyde by intracardiac injection to clear the blood from the vessels. The tumor and surrounding tissue were excised and stored in 10% paraformaldehyde. Paraffin-embedded histological slices (~4  $\mu\text{m}$  thick) were stained with hematoxylin-eosin (H&E). Prussian blue staining was used to identify the iron in the histological sections of the tumor. The samples were deparaffinized and rehydrated, then immersed in a solution containing 5% w/v of potassium ferrocyanide and 10% hydrochloric acid (v/v) in water for 3 h [12]. Slides were rinsed with water and images obtained on a Leica DMR upright microscope (Leica Microsystems, Wetzlar, Germany) equipped with a Retiga EXi Cooled CCD Camera (QImaging, Burnaby, British Columbia, Canada) and Image Pro Plus software (Media Cybernetics, Silver Spring, MD).

## 3. Results

### 3.1 Magnetic nanoparticle characterization

We examined the properties of different pluronic and tetronic block copolymers as surface coatings for our MNPs. The FTIR spectra of each MNP formulation confirmed anchoring of the different types of pluronic and tetronic onto OA coated on iron-oxide core. The block copolymers exhibited broad FTIR bands within the range  $1250\text{ cm}^{-1}$ – $1000\text{ cm}^{-1}$  due to C-O-C stretching and  $\text{CH}_2$  rocking vibrations in the PEO/PPO chains (Fig. 2A). The magnetic cores of the MNPs did not produce a signal in this range. In the FTIR spectra, the characteristic C-O-C and  $\text{CH}_2$  peaks confirm the adsorption of each block copolymer to the MNP surface (Fig. 2B).

We determined the OA and pluronic/tetronic block copolymer content for each MNP formulation by thermogravimetric analysis. Controls included bare MNPs and OA-coated MNPs. Mass loss for all formulations occurred between  $200^\circ\text{C}$  and  $400^\circ\text{C}$ , with the inflection point ranging from  $280^\circ\text{C}$  to  $400^\circ\text{C}$ . The particle composition was predominantly iron-oxide for each formulation (70.1–78.0 weight %, wt%) depending on the copolymer bound, and the OA content ranged from 15.4–17.1 wt%. The copolymer adsorption ranged from 4.9 wt% (L64-modified MNPs) to 14.5 wt% (F127-modified MNPs), Table 2. Generally, as the MW of the PPO increased, a greater percent of copolymer was able to bind to the MNPs. This correlation considers the structure of the PPO (Fig. 1) as copolymers anchor into the OA; the pluronic copolymer will fold in half to anchor onto the OA coating, whereas four equal-sized PPO subunits of the tetronic copolymer will anchor together onto the OA coating around iron-oxide core.

Transmission electron micrographs were similar for all six formulations, with the iron oxide cores measuring ~10–15 nm. The suspending medium greatly influenced MNP size. In water, the hydrodynamic diameter of the MNPs ranged from ~185 to 230 nm for each of the formulations (Table 2). The mean hydrodynamic diameter of Feridex IV was ~140 nm, either in water or PBS, which is smaller than the mean diameter of our MNPs. However, the polydispersity index of our MNPs is significantly lower than that of Feridex IV (polydispersity index = ~0.1 vs. 0.3), suggesting the heterogeneous nature of Feridex IV as compared to our MNPs. Tetronic T904- and pluronic F68- and L64-modified MNPs aggregated in PBS. The MNP size did not change in the presence of BSA. In general, mannitol-citrate buffer was found to be the suitable medium for suspending our MNPs because it did not increase the MNP size significantly compared to MNPs suspended in water.

The binding constants ( $K_b$ ) varied for each MNP formulation (Table 2). Feridex IV and F127-modified MNPs bound strongly to BSA, while T908-modified MNPs bound weakly. The number of binding sites on the MNPs was similar among the formulations (range, 1.15–1.72). Feridex IV and T908-modified MNPs had the highest number of binding sites; pluronic F127-, L64-, and F68-modified MNPs had fewer binding sites.

To determine which MNPs might avoid macrophage premature uptake and clearance *in vivo*, we analyzed MNP uptake in RAW 264.7 cells *in vitro*. Feridex IV uptake was 0.05  $\mu\text{g Fe}/\mu\text{g cell protein}$ , about one fourth as much as any of our MNP formulations. By comparison, macrophage uptake for most pluronic- or tetronic-modified MNPs was about 0.20  $\mu\text{g Fe}/\mu\text{g cell protein}$ . The uptake by macrophages of pluronic F68-modified MNPs was two fold that of the other formulations, with a measured macrophage uptake of 0.48  $\mu\text{g Fe}/\mu\text{g cell protein}$ .

### 3.2 Magnetic resonance imaging

Based on the *in vitro* characteristics of the MNPs, particularly the size and hydrophilic content, we selected F127- and T908- modified MNPs to image in a mouse xenograft tumor model. An initial study confirmed decreased signal intensity and enhanced tumor contrast for F127-modified MNPs immediately after intravenous injection (Fig. 3). The darkened tissue indicating MNP uptake is observed in both the tumor (denoted by arrow) and the liver. Re-injection of the contrast agent at 60 min further decreased the signal intensity. This preliminary study confirmed that the MNPs enhanced the contrast in the tumor tissue. In subsequent experiments, a phantom was placed next to the mouse, the image normalized, and the change in contrast quantified.

The contrast observed within the tumor of mice injected with Feridex IV, T908- or F127-modified MNPs varies at each axial slice due to the heterogeneity of the tumor vasculature (Fig. 4). The decrease in signal intensity is more apparent for each contrast agent in the outer slices of each tumor (Fig. 4, S 02–04 and S 07–08). The contrast in the vascular tumor periphery decreases sharply at 1 h for Feridex IV and T908-modified MNPs and returns to baseline over the next 3 h (Fig. 4 and Supplementary Fig. S3). The reduced signal intensity of the whole tumor in each slice and over the entire volume was not as pronounced for Feridex IV and T908-modified MNPs as with F127-modified MNPs. F127-modified MNPs display enhanced contrast in both the vascular tumor periphery and in whole tumor at 1 h, which persists over the 4 h imaging period (Fig. 4, S All). In addition, F127-modified MNPs were the only particles in which there was a greater decrease in signal intensity in some slices in the whole tumor than in the tumor periphery (Fig. 4, S 03, S 05, and S 06). Mice injected with saline did not show any change in signal intensity over the 4-h imaging period in either tumor periphery or whole tumor.

### 3.3 Histology

Each tumor showed a viable periphery and a necrotic core visible in the H&E-stained sections (Fig. 5). Prussian blue-stained sections indicate iron in the tumor tissue 24 h after injection of the MNPs. The Prussian blue staining appeared only in the tumors of animals that had received MNPs or Feridex IV but not in those of the saline control mice.

## 4. Discussion

The surface properties of MNPs critically influence the interactions of MNPs with proteins, cells, and the localization of MNPs to tumors [6]. To prevent early uptake by macrophages and too rapid clearance of MNPs, the steric stabilization must be optimized so that the polymer used for surface modification is adequately anchored to the surface, the surface is fully coated, and the coating is sufficiently thick [13]. In this study, we analyzed different surface coatings

of our MNPs to limit their clearance by the RES and enhance contrast in xenograft breast tumors. Our study demonstrated that F127-modified MNPs provide whole tumor contrast over an extended time frame of at least 4 h.

Our MNP is composed of an iron-oxide core coated with OA. The OA-magnetite particles are hydrophobic and not dispersible in water. However, this formulation easily allows a hydrophobic/hydrophilic block copolymer to anchor onto the OA-magnetite core for aqueous dispersion (Fig. 1). We modified the surface coating of our MNP formulation with various pluronic and tetronic block copolymers to identify a formulation with minimal protein interaction, extended circulation time, and enhanced uptake into the tumor. We compared our formulations to Feridex IV, a commercial contrast agent.

The steric hindrance of the PPO-PEO subunits and their structural layout was anticipated to influence the ability of the pluronic and tetronic copolymers to anchor onto the OA. The pluronic copolymers (L64, F68, F108, and F127) fold in half to anchor onto the OA; the depth at which the PPO chain can anchor onto the OA is at most one half the overall length of the PPO (Fig. 1). Tetronic T904 and T908 have greater PPO molecular weight than any pluronic (Table 1); however, the copolymer is branched, forming a star shape, allowing tetronic to anchor into the OA a depth of at most one fourth of the overall linear length of the PPO chain (Fig. 1). The PPO chain strengthens the copolymer interaction with the OA-coated MNP, allowing more copolymer to bind and stay bound during MNP synthesis. If the PPO anchoring is inadequate, more of the hydrophobic OA-magnetite core is exposed and the MNPs aggregate.

We determined the size of our MNPs in different media by dynamic light scattering. Compared to Feridex IV, our particles were larger but more monodisperse, i.e. their polydispersity index was smaller than Feridex IV particles. Particles modified with F68, L64, and T904 had a significant increase in size when dispersed in PBS. The increase in size was likely due to the short PPO length available for anchoring, which resulted in low surface coating of these polymers, as confirmed by thermogravimetric analysis (Table 2). This loose anchoring of the above block copolymer may have resulted in their dissociation in the presence of PBS (salting out effect), causing particles to aggregate (Table 2). The overall results suggest that a balance between PPO and PEO chain lengths is essential for anchoring of the block co-polymer via PPO chain on MNPs as well as for their hydration via PEO chain to maintain them in a dispersed state.

Uptake of MNPs by macrophages *in vitro* did not differ significantly among the various pluronic and tetronic copolymers used to coat our MNPs, though they all showed somewhat greater uptake than Feridex IV. Limited PEO and PPO domains significantly influence aggregation, and the large particle size typically leads to increased serum protein adsorption and uptake by macrophages [14]. The PPO chain strengthens the copolymer interaction with the OA-coated MNP, allowing more copolymer to bind and stay bound during MNP synthesis. If the PPO anchoring is inadequate, more of the hydrophobic OA-magnetite core is exposed and the MNPs aggregate.

We selected one pluronic- and one tetronic-coated MNP formulation for *in vivo* MR imaging of the MCF-7 breast tumor in mice. Based on *in vitro* MNP size and copolymer anchoring, F68, L64, and T904 polymers were not considered suitable MNP surface coatings for *in vivo* studies because the RES would too quickly clear the particles. Particles modified with F127 had a very high pluronic content and low number of binding sites compared to F108-modified MNPs, therefore, we selected F127-modified MNPs as the pluronic coated MNP for MRI studies. Tetronic T908-modified MNPs were selected for MRI over T904-modified MNPs because they did not aggregate and had a smaller  $K_b$ , with low macrophage uptake.

In the present study, we took advantage of the defective tumor vasculature for particle accumulation in the tumor, the EPR effect [15]. Other experiments have shown that the EPR effect is an effective means to deliver iron-oxide particles to tumors for MRI, generally with transient accumulation in the first hour followed by clearance of the particles in the next 2 h. Iron-oxide particles modified with poly(ethylene glycol)-poly(aspartic acid) block copolymers or with copolymers thermally cross-linked to the surface of the MNP enhance tumor contrast for 1-3 h or 3.5 h after injection, respectively [16,17]. MRI studies with pegylated gadolinium nanoparticles enhance the contrast in the tumor periphery in the first 40 min, but the contrast fades to that of pre-injection levels 2–6 h post injection [18]. Feridex IV and our T908-modified MNPs paralleled these findings; strong contrast in the tumor periphery 1 h post-injection returned towards baseline by 2.5–3 h post injection. F127-modified MNPs enhanced contrast in the tumor more than T908-modified MNPs and Feridex IV, and the contrast remained for the duration of the imaging.

*In vivo*, the depth of PPO anchoring onto OA may prevent the shear forces the MNPs are exposed to from breaking the physical interaction between the PPO and OA, which may be why the contrast remained for F127-modified MNPs and faded for T908-modified MNPs. In addition, F127-modified MNPs have a much greater wt% of pluronic coating than any of the other MNPs (Table 2) because of the strong PPO anchoring. This increase in the overall wt% of the coating increases the hydrophilic content, which is known to contribute significantly to the extended circulation time [19] by preventing protein adsorption (opsonization) and phagocytosis [20]. This characteristic could explain the transient contrast effect of T908-modified MNPs over F127-modified MNPs because of the difference in their block copolymer content (7.5 wt% for T908-modified MNPs vs. 14.5 wt% for F127-modified MNPs). In addition to extending the circulation time and preventing protein adsorption, phagocytosis, and RES clearance, the stability of the F127-modified MNPs in circulation may also allow the particles to diffuse through the tumor vasculature so that F127-modified MNPs to act as a whole tumor contrast agent. This is a significant improvement compared to the T908-modified MNPs and Feridex IV, which do not show significant whole tumor contrast.

Despite smaller mean size and lower macrophage uptake of Feridex IV compared to our formulation, our previous study [21] showed longer systemic circulation half-life of F127-modified MNPs than Feridex IV in mice (31.2 min vs. 6.4 min). The circulation half-life in the study was determined from the changes in MRI signal intensity in both carotid arteries of mice following a tail vein injection of 7 mg Fe/kg [21]. The longer circulation half-life of F127-modified MNPs than Feridex IV also explains the better tumor contrast seen in this study with F127-modified MNPs.

The rapid clearance of Feridex IV could be due to its heterogeneous particle size distribution compared to F127-modified MNPs (polydispersity index, 0.3 vs. 0.1, Table 2), thus rapidly removing Feridex IV from circulation. Alternatively, the pluronic F127 coating surrounding the iron-oxide core could provide greater particle dispersion stability *in vivo* than the dextran coating used for stabilizing iron-oxide particles in Feridex IV. McCarthy et al. have reported that one of the main drawbacks is that the dextran coating is in equilibrium with the surrounding medium, as it is not strongly associated with the iron oxide core [22]. Additionally, MNPs are subjected to high shear forces *in vivo*, which are not replicated under *in vitro* conditions. Weak binding of the coating agent to the magnetic core could become a critical factor in the destabilization of the formulation when subjected to high shear force *in vivo*. Further studies on the stability of the coating and that of particles under shear force replicating *in vivo* conditions could perhaps provide better insight into the rapid *in vivo* clearance of Feridex IV, which, despite its more favorable characteristics of smaller mean particle size and lower macrophage uptake *in vitro*, did not compare as well to our formulation of MNPs *in vivo*.

We have previously demonstrated the biocompatibility of F127-modified MNPs in rats; the MNPs caused transient changes in the liver enzyme levels or increase in oxidative stress [23]. This finding is important because one of the limitations of the gadolinium-based contrast agents is their serious renal toxicity [24].

The prolonged presence of MNPs in tumors is an advantage not only for MRI, but also to achieve sustained targeted delivery of anticancer drugs, since our formulation has the unique advantage of entrapping high doses of hydrophobic anticancer drugs in the OA layer for sustained release while retaining favorable MRI properties [7,21]. We have previously shown loading of paclitaxel and doxorubicin (base), and also the combination of the two in our MNPs with drug loading of 8.2–9.5 % w/w and sustained release of the loaded drugs [21].

In addition to drug delivery and MRI, MNPs can also be actively targeted to the tumor by conjugating antibodies to the MNPs for receptors over expressed on the cell surface, or by applying an external magnetic field to localize the MNPs to an area of interest [25,26]. The conjugation to a targeting ligand can enhance the efficiency and specificity of MNPs. An alternating magnetic field can be applied to tumor cells containing MNPs to heat and selectively kill cancer cells, which are more sensitive to increased temperature than healthy cells [27]. Targeted nanocarriers with simultaneous imaging and drug delivery capabilities are of clinical importance as it could allow detection of pathologies as well as delivery of therapeutics. Our formulation of MNPs can thus be developed as a theranostic agent with combined properties of drug delivery and imaging

## 5. Conclusions

F127-modified MNPs demonstrated sustained and enhanced contrast throughout the tumor mass, whereas contrast was transient and confined to the tumor periphery with Feridex IV. Since our MNPs can also be loaded with anticancer agents without influencing the MRI properties, these MNPs can be developed as an effective theranostic agent that could potentially be used for tumor detection, drug delivery, and evaluation of response to therapy.

## Supplementary Material

Refer to Web version on PubMed Central for supplementary material.

## ABBREVIATIONS

BSA, Bovine serum albumin  
EPR effect, Enhanced permeation and retention effect  
FTIR, Fourier transform infrared  
H&E, Hematoxylin and eosin  
MRI, Magnetic resonance imaging  
MNPs, Magnetic nanoparticles  
OA, Oleic acid  
PBS, Phosphate-buffered saline  
PEO, Poly(ethylene oxide)  
PPO, Poly(propylene oxide)  
RES, Reticuloendothelial system  
V, Volume

## Acknowledgments

The study reported here is funded by grant R01 EB005822 (to VL) from the National Institute of Biomedical Imaging and Bioengineering of the National Institutes of Health. SPF is a predoctoral student in Cleveland Clinic's Molecular

Medicine Ph.D. Program, which is funded by the “Med into Grad” initiative of the Howard Hughes Medical Institute [<http://www.lerner.ccf.org/molecmed/phd/>]. We thank John Richey for technical assistance with the MRI.

## References

1. Sosnovik DE, Nahrendorf M, Weissleder R. Magnetic nanoparticles for MR imaging: agents, techniques and cardiovascular applications. *Basic Res Cardiol* 2008;103:122–130. [PubMed: 18324368]
2. Weber MA, Giesel FL, Stieltjes B. MRI for identification of progression in brain tumors: from morphology to function. *Expert Rev Neurother* 2008;8:1507–1525. [PubMed: 18928344]
3. Khoo VS, Joon DL. New developments in MRI for target volume delineation in radiotherapy. *Br J Radiol* 2006;79(Spec No 1):S2–S15. [PubMed: 16980682]
4. Frangioni JV. New Technologies for Human Cancer Imaging. *J Clin Oncol* 2008;26:4012–4021. [PubMed: 18711192]
5. Xie J, Xu C, Kohler N, Hou Y, Sun S. Controlled PEGylation of monodisperse Fe<sub>3</sub>O<sub>4</sub> nanoparticles for reduced non-specific uptake by macrophage cells. *Adv Mater* 2007;19:3163–3166.
6. Lode J, Fichtner I, Kreuter J, Berndt A, Diederichs JE, Reszka R. Influence of surface-modifying surfactants on the pharmacokinetic behavior of 14C-poly (methylmethacrylate) nanoparticles in experimental tumor models. *Pharm Res* 2001;18:1613–1619. [PubMed: 11758771]
7. Jain TK, Morales MA, Sahoo SK, Leslie-Pelecky DL, Labhasetwar V. Iron oxide nanoparticles for sustained delivery of anticancer agents. *Mol Pharmaceutics* 2005;2:194–205.
8. Jeffery, GH.; Bassett, J.; Mendham, J.; Denny, RC. Vogel's text book of quantitative chemical analysis. Vol. 5th ed. New York: John Wiley & Sons Inc; 1989.
9. Lehrer SS, Fasman GD. The fluorescence of lysozyme and lysozyme substrate complexes. *Biochem Biophys Res Commun* 1966;23:133–138. [PubMed: 5928904]
10. Chipman DM, Grisaro V, Sharon N. The binding of oligosaccharides containing N-acetylglucosamine and N-acetylmuramic acid to lysozyme. The specificity of binding subsites. *J Biol Chem* 1967;242:4388–4394. [PubMed: 6070843]
11. Horning JL, Sahoo SK, Vijayaraghavalu S, Dimitrijevic S, Vasir JK, Jain TK, et al. 3-D tumor model for in vitro evaluation of anticancer drugs. *Mol Pharmaceutics* 2008;5:849–862.
12. Rodriguez O, Fricke S, Chien C, Dettin L, VanMeter J, Shapiro E, et al. Contrast-enhanced in vivo imaging of breast and prostate cancer cells by MRI. *Cell Cycle* 2006;5:113–119. [PubMed: 16340310]
13. Storm G, Belliot SO, Daemen T, Lasic DD. Surface modification of nanoparticles to oppose uptake by the mononuclear phagocyte system. *Adv Drug Deliv Rev* 1995;17:31–48.
14. Fang C, Shi B, Pei YY, Hong MH, Wu J, Chen HZ. In vivo tumor targeting of tumor necrosis factor- $\alpha$ -loaded stealth nanoparticles: effect of MePEG molecular weight and particle size. *Eur J Pharm Sci* 2006;27:27–36. [PubMed: 16150582]
15. Maeda H, Wu J, Sawa T, Matsumura Y, Hori K. Tumor vascular permeability and the EPR effect in macromolecular therapeutics: a review. *J Controlled Release* 2000;65:271–284.
16. Kumagai M, Imai Y, Nakamura T, Yamasaki Y, Sekino M, Ueno S, et al. Iron hydroxide nanoparticles coated with poly(ethylene glycol)-poly(aspartic acid) block copolymer as novel magnetic resonance contrast agents for in vivo cancer imaging. *Colloids Surf, B* 2007;56:174–181.
17. Lee H, Yu MK, Park S, Moon S, Min JJ, Jeong YY, et al. Thermally cross-linked superparamagnetic iron oxide nanoparticles: synthesis and application as a dual imaging probe for cancer in vivo. *J Am Chem Soc* 2007;129:12739–12745. [PubMed: 17892287]
18. Zhu D, Lu X, Hardy PA, Leggas M, Jay M. Nanotemplate-engineered nanoparticles containing gadolinium for magnetic resonance imaging of tumors. *Invest Radiol* 2008;43:129–140. [PubMed: 18197065]
19. Dunn SE, Coombes AGA, Garnett MC, Davis SS, Davies MC, Illum L. In vitro cell interaction and in vivo biodistribution of poly(lactide-co-glycolide) nanospheres surface modified by poloxamer and poloxamine copolymers. *J Controlled Release* 1997;44:65–76.

20. Besheer A, Vogel J, Glanz D, Kressler J, Groth T, Mader K. Characterization of PLGA nanospheres stabilized with amphiphilic polymers: Hydrophobically modified hydroxyethyl starch vs pluronics. *Mol Pharmaceutics* 2009;6:407–415.
21. Jain TK, Richey J, Strand M, Leslie-Pelecky DL, Flask CA, Labhasetwar V. Magnetic nanoparticles with dual functional properties: Drug delivery and magnetic resonance imaging. *Biomaterials* 2008;29:4012–4021. [PubMed: 18649936]
22. McCarthy JR, Weissleder R. Multifunctional magnetic nanoparticles for targeted imaging and therapy. *Adv Drug Deliv Rev* 2008;60:1241–1251. [PubMed: 18508157]
23. Jain TK, Reddy MK, Morales MA, Leslie-Pelecky DL, Labhasetwar V. Biodistribution, clearance, and biocompatibility of iron oxide magnetic nanoparticles in rats. *Mol Pharmaceutics* 2008;5:316–327.
24. Hasebroock KM, Serkova NJ. Toxicity of MRI and CT contrast agents. *Expert Opin Drug Metab Toxicol* 2009;5:403–416. [PubMed: 19368492]
25. Peng XH, Qian X, Mao H, Wang AY, Chen ZG, Nie S, et al. Targeted magnetic iron oxide nanoparticles for tumor imaging and therapy. *Int J Nanomedicine* 2008;3:311–321. [PubMed: 18990940]
26. Alexiou C, Jurgons R, Seliger C, Brunke O, Iro H, Odenbach S. Delivery of superparamagnetic nanoparticles for local chemotherapy after intraarterial infusion and magnetic drug targeting. *Anticancer Res* 2007;27:2019–2022. [PubMed: 17649815]
27. Wiekhorst F, Seliger C, Jurgons R, Steinhoff U, Eberbeck D, Trahms L, et al. Quantification of magnetic nanoparticles by magnetorelaxometry and comparison to histology after magnetic drug targeting. *J Nanosci Nanotechnol* 2006;6:3222–3225. [PubMed: 17048540]

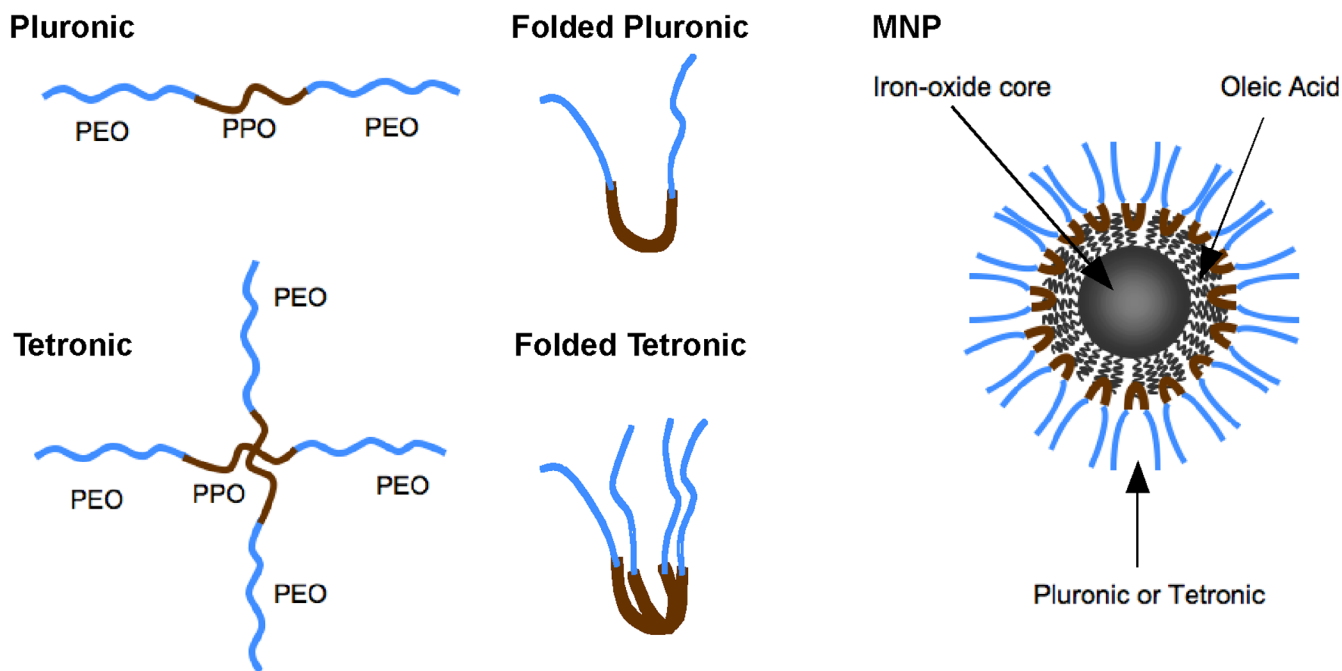


**Fig. 1.** Schematic of MNPs. Each particle contains an iron-oxide core coated with OA and is coated with either pluronic (single PEO-PPO-PEO subunit) or tetronic (two PEO-PPO-PEO subunits). The PPO subunit from the copolymers adsorbs onto the OA rendering the MNPs dispersible in aqueous solution. (Pluronic and tetronic are registered trademarks of BASF SE, Ludwigshafen, Germany.)

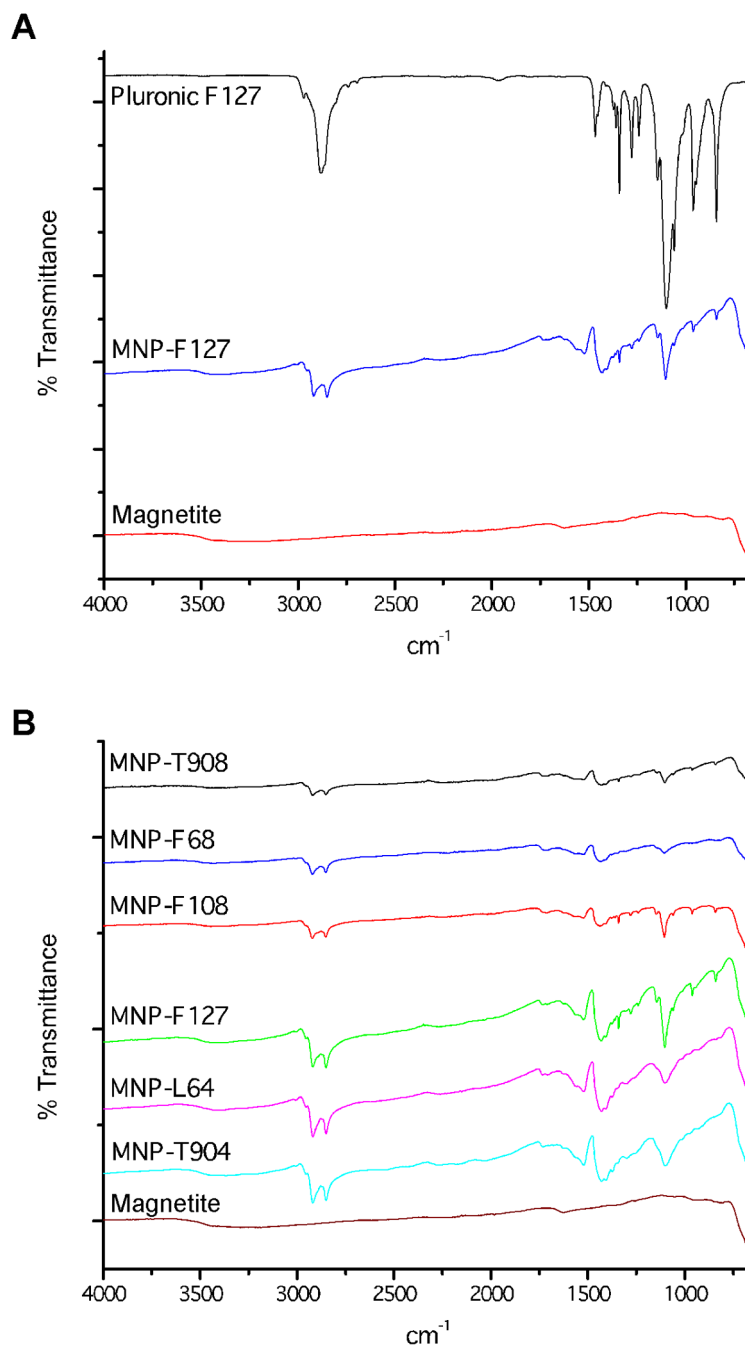


**Fig. 2.** Characterization of anchoring of pluronic or tetronic to the OA coated MNP. **A**, FTIR peaks characteristic for pluronic F127 are present on F127-modified MNPs and not OA-magnetite core confirming adsorption of the pluronic to the magnetite core. **B**, Peaks for the C-O-C and  $\text{CH}_2$  functional groups of pluronic and tetronic copolymers confirm that each of the six copolymers anchors onto the magnetite particle.

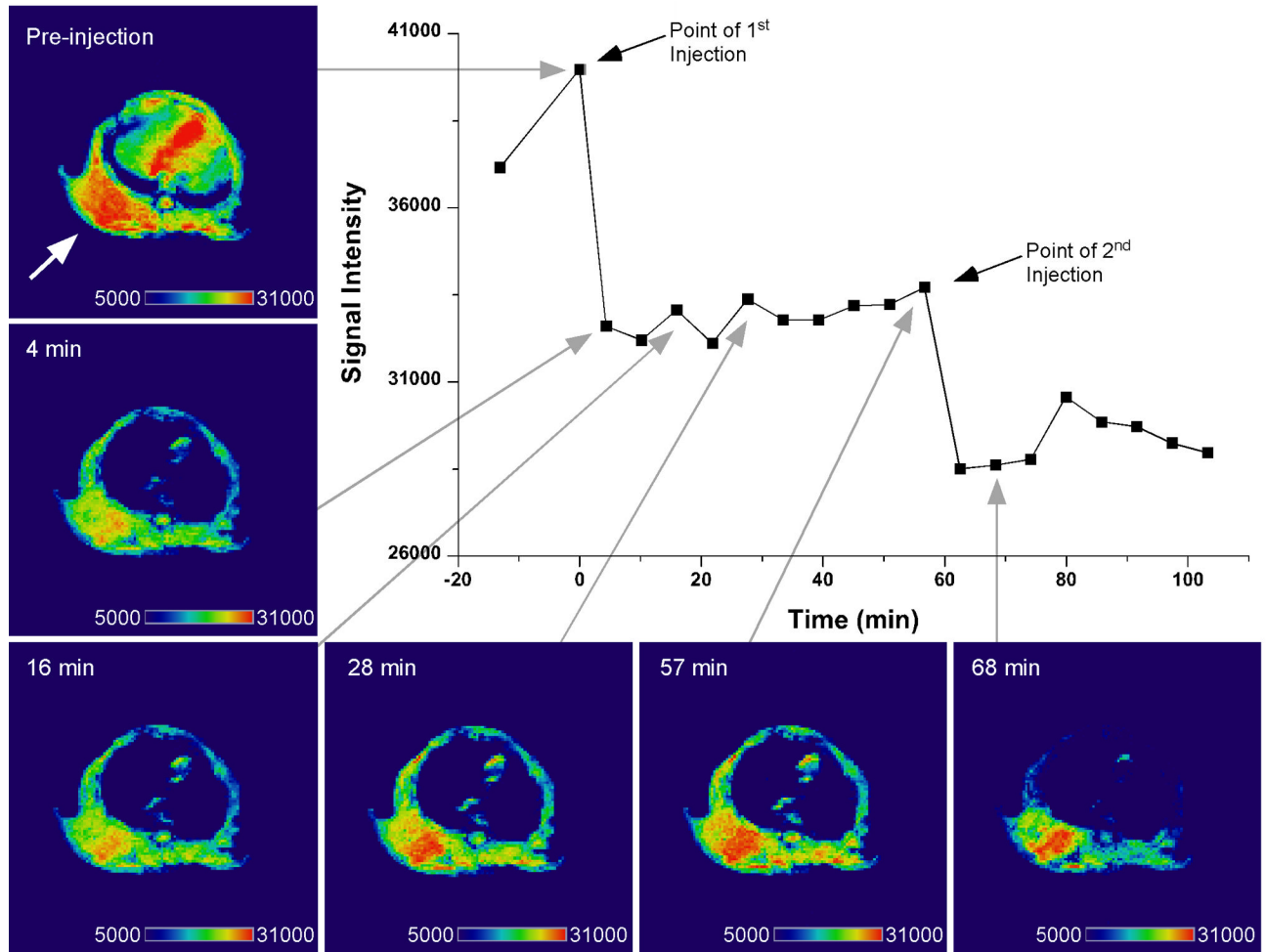


**Fig. 3.** T<sub>2</sub>-weighted image of tumor bearing mouse injected with pluronic F127-modified MNPs. Enhanced contrast in the tumor (denoted by arrow) is apparent 4 min after the initial injection and is more pronounced at 68 min after a second injection of the MNPs. Images were analyzed for signal intensity in the tumor with Amira software (Visage Imaging, Inc., San Diego, CA).

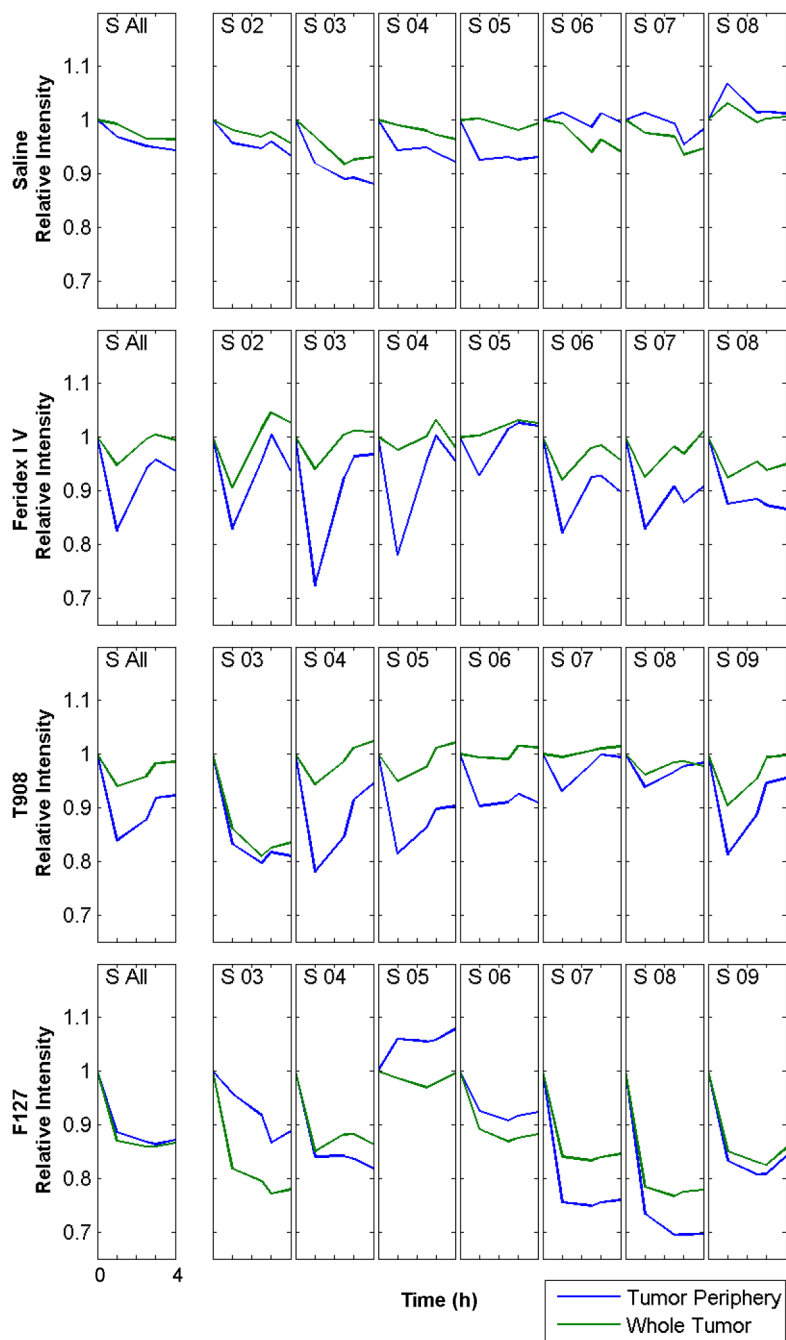


**Fig. 4.**

MNPs taken up within the tumor tissue enhance MRI contrast. Contrast enhancement within the whole tumor and vascular tumor periphery for mice injected with saline, Feridex IV, F127-modified MNPs, or T908-modified MNPs. A single ROI was drawn around the tumor at each axial slice (S 02–S 09) for the pre-injection image (0 h) and the signal intensity quantified. The same ROI was used to calculate the signal intensity at 1, 2.5, 3 and 4 h. The signal intensity from a second ROI drawn just inside the first was subtracted from the first to determine the signal intensity within the tumor periphery. An area weighted average of the slices gave the signal intensity for the whole tumor (S All). X-axis: each tick mark represents 1 h, beginning

at 0 h and ending 4 h post injection of saline or the iron-oxide contrast agent. Images analyzed in MATLAB (The MathWorks, Natick, MA). Data represented from at least two repeats.

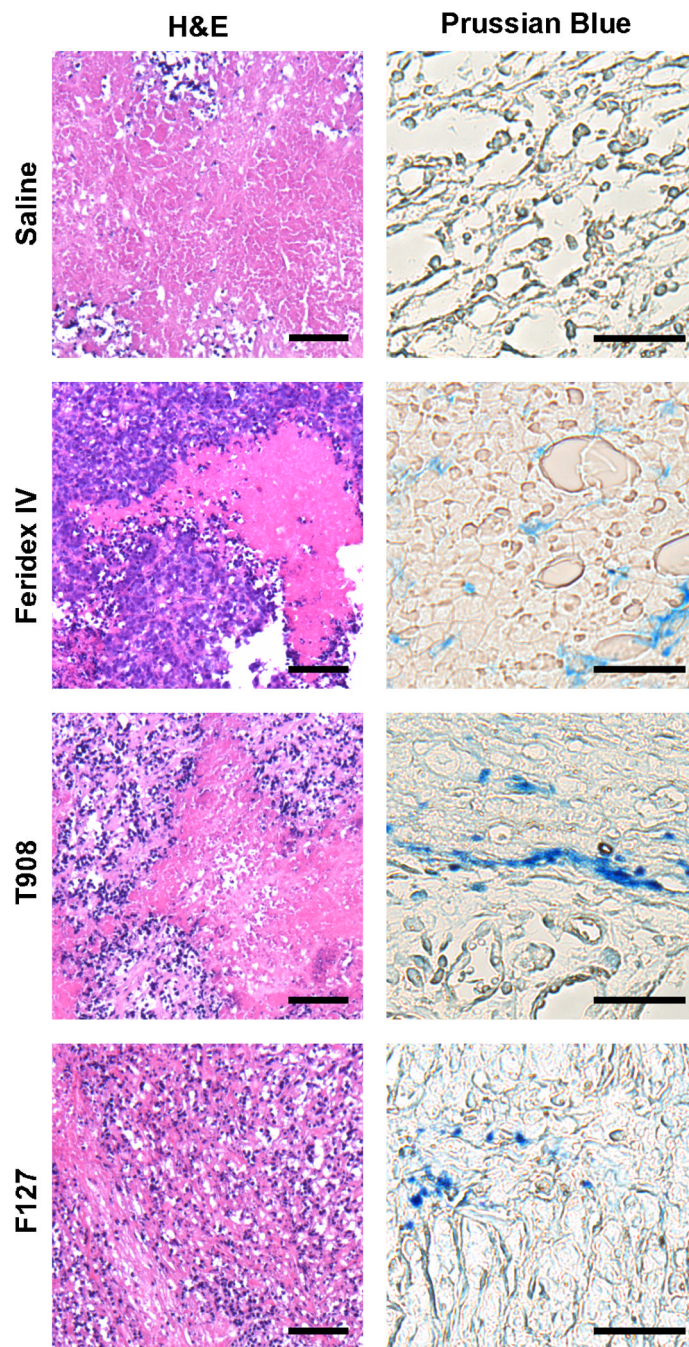


**Fig. 5.** Tumor histological analysis after injection with iron-oxide contrast agents. Blue-violet staining of the viable periphery and red-pink staining of the necrotic core is evident in each H&E-stained tumor section. Iron from the MNPs stained blue in the tumor periphery 24 h after MNP injection. The scale bars are 25  $\mu\text{m}$  in all H&E-stained images, and 10  $\mu\text{m}$  in all Prussian Blue-stained images.

**Table 1**  
Properties of Pluronic and Tetronic block copolymers used to coat MNPs

Co-polymer	Formula	Molecular weight		
		% PEO	PPO	HLB
Pluronic F68	H(EO) <sub>76</sub> (PO) <sub>29</sub> (EO) <sub>76</sub>	80	1680	29
Pluronic F108	H(EO) <sub>133</sub> (PO) <sub>50</sub> (EO) <sub>133</sub>	80	2920	27
Pluronic F127	H(EO) <sub>100</sub> (PO) <sub>65</sub> (EO) <sub>100</sub>	70	3780	22
Pluronic L64	H(EO) <sub>13</sub> (PO) <sub>30</sub> (EO) <sub>13</sub>	40	1740	15
Tetronic 904	[–CH <sub>2</sub> N[(PO) <sub>17</sub> –(EO) <sub>15</sub> H] <sub>2</sub> ]	40	4020	12–18
Tetronic 908	[–CH <sub>2</sub> N[(PO) <sub>22</sub> –(EO) <sub>14</sub> H] <sub>2</sub> ]	80	5000	>24

PEO, poly(ethylene oxide); PPO, poly(propylene oxide); HLB, hydrophilic-lipophilic balance.

Effect of Pluronic and Tetronic coatings on MNP characteristics *in vitro*

Table 2

Co-polymer	% Co-polymer bound to MNPs	Protein binding		Macrophage uptake ( $\mu\text{g Fe}/\mu\text{g cell protein}$ )	Diameter of MNPs (nm) and (Polydispersity Index)			
		$K_b$	$n$		Water	Mannitol citrate buffer	PBS	BSA after 4 h
Feridex IV	—	0.111	1.58	0.051	143 (0.29)	—	126 (0.28)	113 (0.29)
Pluronic F68	6.0	0.046	1.39	0.477	216 (0.12)	255 (0.08)	340 (0.14)	224 (0.08)
Pluronic F108	8.6	0.090	1.55	0.168	206 (0.09)	248 (0.11)	277 (0.17)	223 (0.08)
Pluronic F127	14.5	0.094	1.15	0.222	194 (0.10)	238 (0.08)	257 (0.15)	228 (0.15)
Pluronic L64	4.9	0.082	1.38	0.202	186 (0.10)	243 (0.13)	539 (0.46)	220 (0.12)
Tetronic 904	8.5	0.075	1.48	0.198	196 (0.15)	215 (0.12)	321 (0.21)	202 (0.15)
Tetronic 908	7.5	0.036	1.72	0.190	228 (0.11)	253 (0.11)	257 (0.13)	236 (0.06)

\* Co-polymer bound to MNPs was determined by thermogravimetric analysis.

\*\* 0.1 mg/ml particles incubated with the mouse leukemic monocyte macrophage cell line RAW 264.7.

\*\*\* Particle size measured following 4 h incubation in the presence of 100  $\mu\text{g/ml}$  BSA in water. Particle size represents hydrodynamic diameter. Core diameter (measured using transmission electron microscopy) was 10–15 nm. MNPs have negative zeta potentials, typically ranging from  $-20$  to  $-30$  mV.

MNPs, magnetic nanoparticles, PBS, phosphate-buffered saline; BSA, bovine serum albumin.